



An experimental study of shock transmission from a detonation tube

J. C. Thomas¹ · F. A. Rodriguez¹ · D. S. Teitge¹ · L. N. Kunka² · G. N. Gaddis² · Z. K. Browne¹ · C. B. Ahumada¹ · E. T. Balci² · S. I. Jackson² · E. L. Petersen¹ · E. S. Oran²

Received: 26 October 2021 / Revised: 6 April 2022 / Accepted: 26 May 2022 / Published online: 18 July 2022
© The Author(s), under exclusive licence to Springer-Verlag GmbH Germany, part of Springer Nature 2022

Abstract

An experimental evaluation of the transmission of shock waves from a detonating gas mixture in a 0.5-in-inner-diameter open-ended tube into an inert atmosphere is described in this paper. Stoichiometric H₂/O₂ at 1 atm was used as the reactive gas medium. Results from in-tube diagnostics indicated successful deflagration-to-detonation transition (DDT), which leads to an overdriven detonation before exiting the tube at near Chapman–Jouguet (CJ) conditions. Out-of-tube diagnostics characterized the transmission of the shock wave into the surrounding environment, where the shock wave decays into an acoustic wave as it travels away from the tube exit. A mathematical treatment of overpressure and time-of-arrival data allowed for a direct analytical description of the transmitted shock wave's transient velocity. This description is combined with a first-principles gas-dynamics treatment of the moving normal shock wave to describe the conditions behind the attenuating shock wave. This work furthers the understanding of shock transmission from an open-ended detonation tube and provides a theoretical framework to estimate the resulting conditions.

Keywords Detonation · Shock wave · Decay · Acoustics

1 Introduction

Transmission of a shock wave from a detonation propagating inside of a tube into an open atmosphere is an engineering problem relevant to many applications, such as process safety analysis and pulse detonation engines (PDEs). Experiments were performed in this study to gain a better fundamental understanding of the conditions outside of the open end of a tube when detonation waves propagate from it and into the surrounding atmosphere. There are several components to this problem. Ignition of a reactive gas mixture in a confined tube yields flame acceleration that leads to a deflagration-to-detonation transition (DDT) and an overdriven detonation that decays to a Chapman–Jouguet (CJ) detonation. The detonation wave transmits a shock wave into the surrounding atmosphere at its open end, and the shock wave velocity is

dependent on the acoustic properties of the combustible mixture and the inert mixture in the surrounding atmosphere. The transmitted shock wave decreases in strength as it moves away from the tube opening and eventually decays to an acoustic wave traveling at the local speed of sound.

There is considerable documentation of detonations and DDT in the literature. We know that DDT is due to the complex interaction of flames, shocks, boundary layers, and turbulence which include both gas-dynamic and chemical processes [1]. Transmission of a shock wave from a detonating medium into a separate medium has also been studied in the literature. Several researchers have considered a detonation-driven shock tube as an experimental tool [2–12]. In this case, the driven section contains a detonable mixture and is separated from the driver section by a thin diaphragm. The detonation yields a significant pressure increase which ruptures the diaphragm and transmits a shock wave through the driver section. However, most of these facilities operate in the “upstream-propagation” mode in which detonation is directly initiated near the diaphragm, rather than allowing a detonation to reach the diaphragm (e.g., “downstream-propagation” mode) [6,7]. Morrison [2] derived a first-principles treatment of the downstream-propagation mode but did not provide experi-

Communicated by G. Ciccarelli.

✉ J. C. Thomas
James.Chris.Thomas@tamu.edu

¹ J. Mike Walker '66 Department of Mechanical Engineering, Texas A&M University, College Station, TX, USA

² Department of Aerospace Engineering, Texas A&M University, College Station, TX, USA

mental validation of the model. Armstrong [10] described a numerical CFD model of this phenomenon which is an approach that shows potential for predictive capability.

Several researchers have also considered the transmission of a shock wave from the surface of a condensed-phase explosive [13,14], a phenomenon with considerable similarities to the current problem. Thomas et al. [15] studied the transmission of shock waves from detonating gases through inert mediums (He, Ar, air, and CO₂) and concentration gradients, and their data were compared to theory presented by Paterson [14]. Sochet et al. [16] studied shock wave transmission into atmospheric air from detonating gaseous mixtures (propane or hydrogen with oxygen) constrained to hemispherical and half-tube geometries. These studies included near- and far-field overpressure measurements and provided a scaling analysis based on piston or bulk energy models. Kato et al. [17] performed similar experiments with ethylene and oxygen constrained to a tubular geometry. In addition, Kato et al. [17] provided scaling analysis comparisons to the data of Sochet et al. [16] and similar shock-tube experiments [18,19]. Several other research groups [20–26] have also considered this problem due to its applicability in PDEs.

Pack [27] was among the first to recognize that transmission of the shock wave from the detonating medium depends on the relative acoustic impedances of each medium. Recently, Peace and Lu [28] studied shock wave transmission in a downward-propagating detonation-driven shock tube over a range of impedance ratios, where the reactive and inert mediums consisted of hydrogen/oxygen and air/helium. Peace and Lu [28] also developed a theoretical shock transmission model which included the effects of the leading shock, induction zone, and reaction zone.

No fully descriptive model has been presented to date that accurately captures the overpressure decay behind a shock wave transmitted into an open volume from a detonation inside of a tube. Allgood [20] and Glaser et al. [21] suggested that the pressure in the near and far fields due to the shock wave exiting a PDE could be represented by standard scaling correlations for strong and weak shocks, respectively, but only approximate agreement with their data is noted. Anand et al. [25] later applied an empirical correlation developed by Dorofeev et al. [29] for hemispherical detonations to their PDE overpressure decay data and noted good agreement if the correlation was scaled by an empirical factor of 3.43. The observed level of disagreement between data presented from the two studies without this scaling factor is not surprising, considering the differences in their explosion geometry and how each group defined their explosion energy. The limited available data and the lack of a comprehensive model highlight the need for an additional investigation of this phenomena.

In summary, shock wave transmission from a detonating medium into an open volume has been documented in the

literature, but the intricacies of the complex interacting phenomena involved and how they affect the resultant attenuating shock wave require further investigation. The current work provides experimental data and corresponding analysis and therefore a better understanding of these phenomena. The following section provides an overview of the experimental configuration, including detonation tubes, gas handling systems, and instrumentation used for data acquisition. Representative data and data reduction methods are subsequently provided. A detailed analysis of the shock wave decay data is presented alongside the development of an analytical model. Finally, key findings and areas of future work are discussed in Conclusions section.

2 Experimental methods

2.1 Experiment overview

The open-ended detonation-tube facility is shown in Figs. 1 and 2. These figures provide a detailed schematic of the gas handling system and an image of the assembled experiment, respectively. The experiment consists of three open-ended detonation tubes connected to a gas delivery system, instrumentation, and a DAQ/control box. Only experiments from the smallest detonation tube are presented and discussed here. This tube has an inner diameter of 0.5 in (1.27 cm) and a maximum length of 5 ft (1.52 m). The detonation tube is constructed from flanged sections, such that its total length can be adjusted within 1-ft (0.3-m) increments. The end of the tube is terminated with a blind flange that includes a pressure-sealed insert housing a Nichrome ignition wire, which is connected to a circuit containing a relay and a variable power supply (VolTEQ #HY3020EX). The tube is secured on top of leveled cinderblocks during experiments, and its outer diameter rests approximately 1 ft (0.3 m) above the ground.

The gas delivery system (Fig. 1) controls the flow of fuel, oxidizer, and reactive gas mixtures in the manifold and to the detonation tube. Four tanks are connected to the manifold for oxidizer (O₂), fuel (H₂), purge gas (N₂), and air for pneumatic valve control. High-pressure dual-stage regulators (Matheson SEQ3128AXXX) are connected to the oxidizer, fuel, and purge gas tanks. Two programmable mass flow controllers (Alicat #MCP-100SLPM-D) are installed in-line downstream of the oxidizer and fuel tanks for precise control of their flows. Fuel and oxidizer mixing takes place in-line prior to entry into the detonation tube. A single detonation arrestor (Protego DAL-1/4-IIC-P1.5) is installed just upstream of the detonation tube. Three high-pressure pneumatic valves (HiP 10-11NFB-MH-NC) are used to remotely control the flow of the reactive gas mixture into the detonation tube and gas analyzer (CAI GPA2000) and to

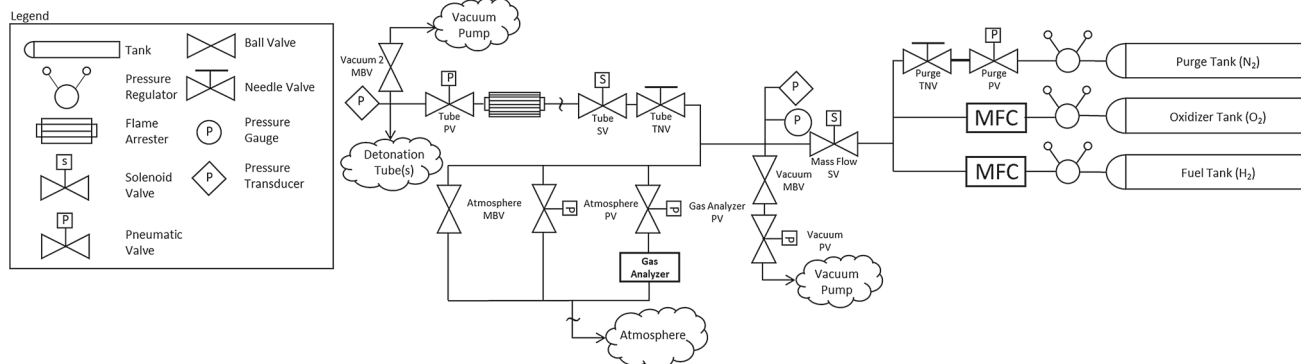


Fig. 1 Detailed schematic of the gas handling system including gas tanks, mass flow controllers, pneumatic valves, static pressure transducers and gauges, detonation arrester, and vacuum pumps. The air tank and corresponding lines for pneumatic control are not depicted

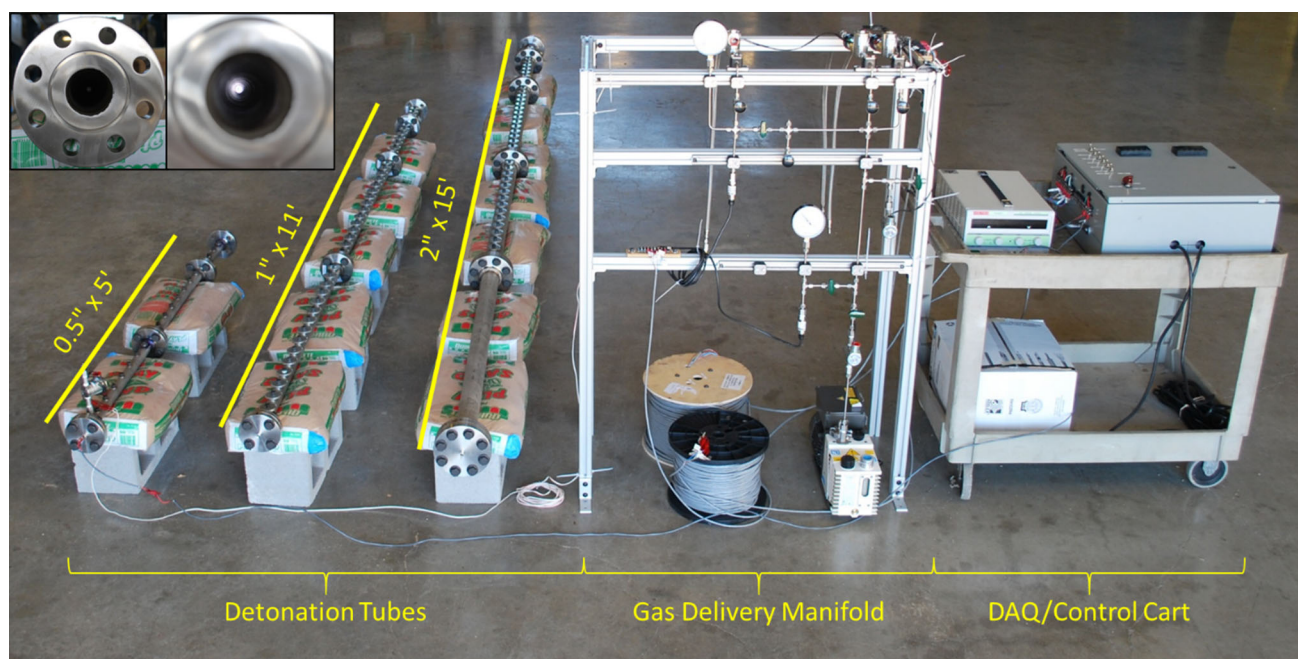


Fig. 2 Image of all three fully assembled detonation tubes, gas handling system, and deployable DAQ/control cart. Inset images show end views of the 5.08-cm (2-in) tube

control flow of the purge gas. Three high-pressure solenoids (Peter Paul Electronics #H22M9DCV) remotely control flow to the atmosphere vent line and the vacuum pumps. Additional valving allows for manual venting. Two separate rotary vane pumps (Agilent DS102) are used to remove gas in the gas delivery manifold and detonation tube. The gas manifold contains a pressure gauge (AshCroft #355-10) and two pressure transducers (Omega #PX309-300A5V and Omega #PX309-050A5V) to actively monitor the gas manifold and detonation-tube conditions.

The length of the detonation tube contains ports along its centerline for instrumentation. The inter-port spacing is approximately 3 in (7.6 cm). A 30-in (76-cm) long pressure

transducer rake (Fig. 3) is mounted at the tube exit, flush with the exit's outer diameter, and can house up to 19 sensors. High-frequency, high-resolution, ground-isolated, ablative-coated piezoelectric pressure sensors (PCB #CA102B) were used to measure pressure-histories behind the detonation wave inside of the tube and behind the shock wave propagating into the atmosphere. A total of 16 pressure transducers including (6) 0–500 psia, (3) 0–200 psia, (3) 0–100 psia, and (4) 0–50 psia models were utilized during each experiment. Additionally, four free-field, pre-polarized, pre-amplified microphones (PCB #377C01) were set up in the field away from the detonation tube to measure acoustic wave strength behind the wave propagating into the atmosphere. Standard

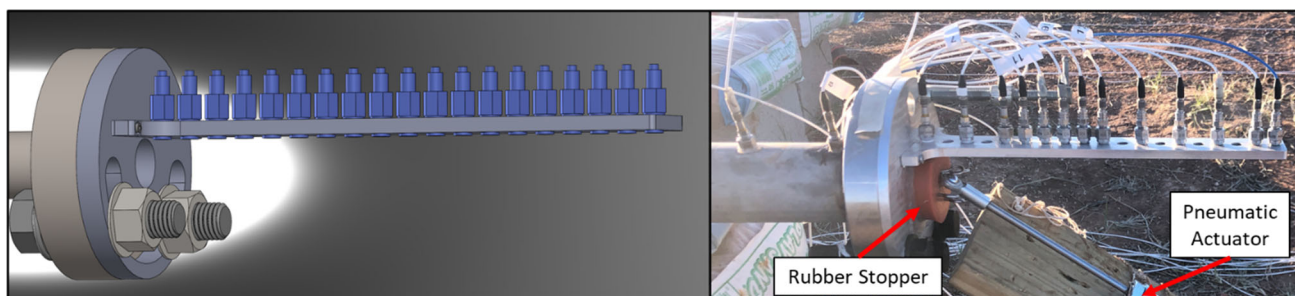


Fig. 3 (Left) CAD representation and (right) image of the pressure transducer rake utilized to secure piezoelectric pressure transducers near the exit of the detonation tube

coaxial data cables with FEP jackets (PCB #002AC) connect all sensors to the DAQ (HBM 1-Gen3i, 3 18-bit GN815 data cards, 200 MS/s, 480 GB SSD). The typical instrumentation configuration in the current study consisted of 4–6 dynamic pressure transducers mounted along the length of the detonation tube, 10–12 dynamic pressure transducers mounted in the rake, and four free-field microphones set up in the field at various distances (2.5–25 m) from the detonation tube. In addition, a standard video camera and a high-speed camera (Photron FASTCAM SA3 120K) captured shock wave and jet flame transmission in select experiments.

2.2 Testing protocol

All experiments took place outdoors at TAMU's UXO Range at the RELIS campus, where operators were located a safe distance (~ 250 m) away from the experiment during reactive gas mixing, filling, and firing operations. Prior to testing, the open end of the detonation tube was plugged with a tapered rubber stopper that minimally (< 1 cm) penetrated the inside of the tube. A pneumatic linear actuator was secured to the stopper to hold it in place (Fig. 3). This method was developed to minimize the impact of the seal on shock wave transmission and was superior to other methods explored here (e.g., plastic diaphragms, thin films, unremoved stoppers). The gas manifold, detonation tube, and associated piping were vacuumed down to a value of 0 psia (pressure readout resolution is 0.1 psia), and a vacuum was continually pulled for an additional 10 min. The detonation tube was filled with reactive gas up to atmospheric pressure and then sealed off from the rest of the system. The gas manifold and connecting piping were vented, purged with nitrogen gas, and vacuumed down to isolate the reactive gas mixture in the detonation tube. The experiment was initiated by removing the rubber stopper by triggering the pneumatic linear actuator and subsequent application of an electrical current to the Nichrome wire igniter. The DAQ system was automatically triggered by arrival of the detonation wave at the exit of the detonation tube.

3 Results and discussion

3.1 Data reduction (in-tube diagnostics)

In a smooth tube, a flame acceleration phase followed by the onset of detonation and subsequent decay of an overdriven detonation to a CJ detonation has been well described in the literature [30]. To verify the presence of a CJ detonation wave at the tube exit, the tube length was varied among three values of 0.6, 0.9, and 1.5 m (2, 3, and 5 ft.), and the six highest-range dynamic pressure transducers (0–3.45 MPa, 0–500 psi) were moved along the length of the tube between experiments. The maximum raw overpressure data collected during these experiments are shown in Fig. 4a as a function of distance from the ignition location (i.e., the closed end of the tube). Similarly, the average wave velocity measured between sensors is shown in Fig. 4b. The average wave velocity between two sensors is defined as the distance between the sensors divided by the difference in wave arrival time. Each of the nine sets of symbols correspond to a separate experiment. The different symbol shapes represent duplicate experiments, while different filling patterns represent different tube lengths. The dashed lines in Fig. 4 correspond to the CJ detonation values for stoichiometric H_2/O_2 . For the maximum overpressure values reported for sensors near the ignition source (e.g., the first two sensors), care was taken to report the pressure associated with the pre-DDT deflagration and not the retonation wave. The measurement errors for maximum pressure (± 50 kPa) and wave velocity (± 50 m/s) are both on the order of the symbol size shown in Fig. 4. The anticipated trend is observed, with DDT occurring near the closed end of the tube after an acceleration phase, yielding an overdriven detonation that decays to near-CJ conditions. Stable conditions, with pressures and wave velocities near the expected CJ conditions, are observed at the open end of the detonation tube.

The experimental overpressure data near the DDT event ($P_{\max} \sim 3.38$ MPa, 490 psi) are significantly higher than the CJ value ($P_{CJ} = 1.90$ MPa, 276 psi), while the wave velocity goes to the CJ value ($V_{CJ} = 2.84$ km/s) almost immediately.

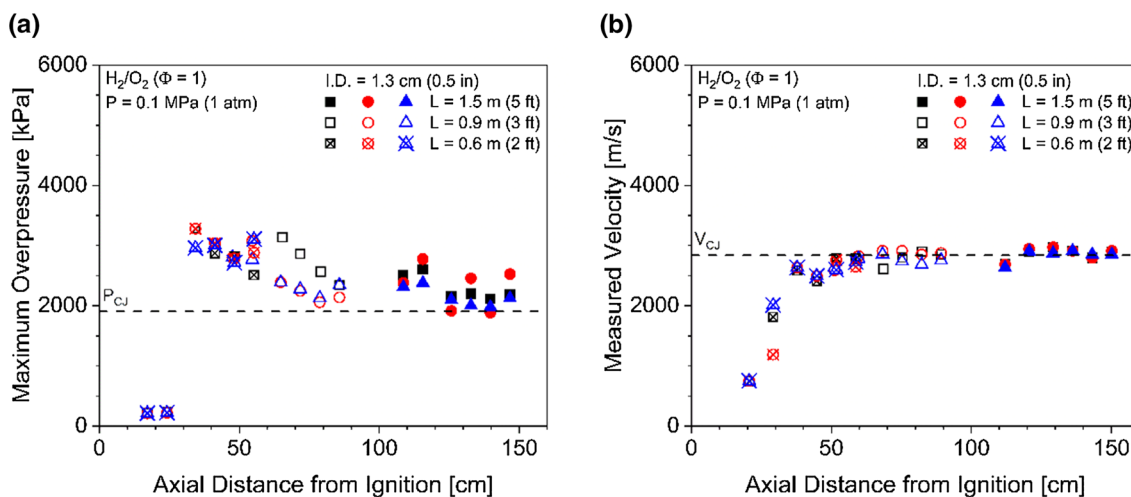


Fig. 4 **a** Maximum overpressure data and **b** computed wave velocities inside of the detonation tube (ID = 1.27 cm, $L = 0.6, 0.9,$ or 1.5 m) for a total of nine experiments conducted with stoichiometric H_2/O_2

($P = 0.1$ MPa). Symbol shapes represent replicate experiments, while different filling patterns represent different tube lengths

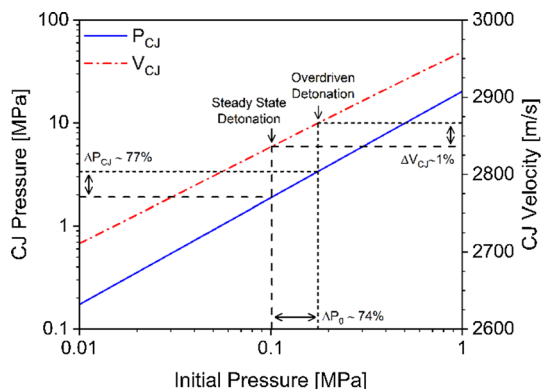


Fig. 5 Initial pressure-dependent CJ detonation properties (CJ detonation pressure and velocity) of stoichiometric H_2/O_2

In contrast, previous investigations by Ciccarelli et al. [31] showed that both the local overpressure and wave velocity exhibit similar behavior in H_2 /air/steam mixtures, in that they are significantly higher than the CJ value near the DDT event and then trend to the CJ value. The authors attempt to rectify this disparity by considering the theoretical CJ conditions of stoichiometric H_2/O_2 detonating at varying initial pressures, as shown in Fig. 5. The stoichiometric H_2/O_2 CJ velocity does not significantly depend on the initial pressure, while the CJ pressure does strongly depend on the initial pressure. More explicitly, the pressure amplification required to yield the observed maximum pressure near the DDT event is an initial reactive gas pressure of approximately 0.177 MPa, which is 74% greater than the standard pressure (0.1 MPa). This overdriven condition yields an increase in the CJ pressure of 77%, but the corresponding increase in the CJ velocity is only 1%. The sensor spacing used here does not allow for high spatial resolution of the local post-detonation conditions, so observation of an increased wave velocity is

difficult and is probably only realizable with other measurement methods, such as direct high-speed video observations. These observations should be considered in future experiments when making measurements of DDT location and run-up distances. Furthermore, it would be worthwhile to perform similar calculations for other fuel/oxidizer mixtures to see if these observations are universal or only applicable to H_2/O_2 mixtures.

3.2 Data reduction (out-of-tube diagnostics)

Representative data for a stoichiometric H_2/O_2 mixture undergoing DDT and transmitting a shock wave into the open atmosphere are shown in Fig. 6 for a detonation tube with ID = 1.27 cm and $L = 1.52$ m. Six pressure transducers were located inside of the tube near its open exit, ten pressure transducers were located in the rake outside but near the tube exit, and four free-field microphones were located away from and in line with the tube exit. The left and right profiles in Fig. 6 correspond to data for the piezoelectric transducers (PZT) and free-field microphones, respectively, and the dashed red line in the left plot corresponds to the arrival of the detonation wave or shock wave. The maximum raw overpressure measured inside of the detonation tube was 2.38 MPa (345 psi), which is greater than the Chapman–Jouguet (CJ) pressure for the mixture of 1.90 MPa (276 psi). However, the measured overpressure decayed inside of the tube and was steady in the region near the tube exit to a value within about 10% of the CJ pressure (2.2 ± 0.18 MPa), indicating a CJ detonation wave had developed. The overpressure signal just outside of the tube exit (i.e., 1.27 cm away) registered a significantly lower value of 1.09 MPa (157 psi), and the overpressure continued to decrease as the shock wave moved away from the tube exit

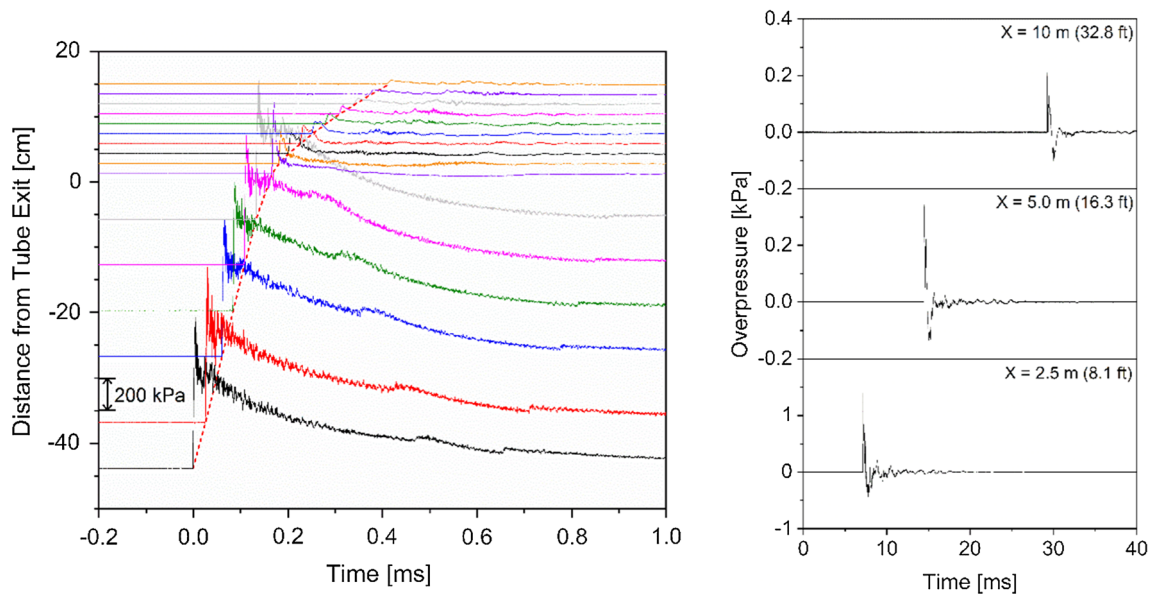


Fig. 6 Representative data collected by the (left) PZT pressure and (right) free-field microphone sensors during a stoichiometric H_2/O_2 detonation tube (ID = 1.27 cm, $L = 1.52$ m) firing

and into the surrounding atmosphere. The furthest pressure transducers in the rake ($D = 15.0$ cm) registered an overpressure of 61 kPa (8.9 psi). The free-field microphones, which are located significantly further from the tube exit at distances ranging from 2.5–25 m, registered overpressures on the order of 1.4–6.9 kPa (0.2–1 psi), and the furthest microphone ($D = 17.4$ m) did not register an overpressure signal greater than the signal noise resolution (0.69 Pa or 0.0001 psi).

We do not expect the pressure rake to influence the peak shock pressure or the decay of the shock wave. However, the rake may have some influence on how fast local pressure conditions return to pre-shock wave values and the corresponding measured impulse.

3.3 Wave decay analysis

The CJ detonation transmits a shock wave at the tube exit at an initial velocity (V_e), and this shock wave decays to an acoustic wave traveling at the ambient speed of sound (c) far from the tube exit. The transmitted shock wave's time-of-flight data (Fig. 7) can be mathematically represented by an oblique asymptote:

$$D(t) = (a_1 t + a_2) - \left\{ \frac{a_3}{t + a_4} \right\} \quad (1)$$

where D is the distance from the tube exit and t is the elapsed time since the detonation wave reached the tube exit. Equation (1) can be differentiated with respect to time to yield the velocity time-history of the shock wave:

$$V(t) = \frac{\partial D}{\partial t} = a_1 + \frac{a_3}{(t + a_4)^2}. \quad (2)$$

The relevant constants of the oblique asymptote equations (i.e., a_1 – a_4) can be solved for by considering the problem's physical constraints at the boundaries. In particular, the tube exit is defined as the shock wave origin: $D(0) = 0$, the initial shock wave velocity at the tube exit is known: $V(0) = V_e$, and the shock wave velocity far away from the tube is equal to the local speed of sound: $\lim_{t \rightarrow \infty} V = c$. In addition, we define an empirical decay coefficient, D_0 , which describes how rapidly the shock wave decays to the local speed of sound. The asymptote of the shock wave time-of-flight data is described by:

$$D(\text{asymptote}) = ct + D_0. \quad (3)$$

Finally, the shock wave location and velocity can be recast:

$$D(t) = (ct + D_0) - \left\{ \frac{D_0^2 / (V_e - c)}{t + [D_0 / (V_e - c)]} \right\} \quad (4)$$

$$V(t) = \frac{\partial D}{\partial t} = c + \frac{D_0^2 (V_e - c)}{[D_0 + (V_e - c)t]^2} \quad (5)$$

where there are three unknown parameters (c , D_0 , and V_e) that must be determined.

The ambient speed of sound can be determined prior to experiments based on local conditions (pressure, temperature, and humidity), but is directly measured here by fitting a line through the time-of-arrival data collected with the far-field microphones. It is worth noting that the ambient speed

of sound varied between testing days throughout the year, and measured values generally agreed well with theoretical values computed according to recorded ambient conditions.

The velocity of the shock wave at the tube exit is found by considering the impedance ratio between the combustible and ambient gases. Peace and Lu [28] investigated the transmission of a shock wave produced by a CJ detonation (H_2/O_2 , $\phi = 0.5-1.5$, $P = 1$ atm) into inert media (air and/or He) with varying acoustic impedance characteristics. They found that the transmitted shock can be amplified or attenuated based on the ratio of acoustic impedances across the contact surface. The nondimensional acoustic impedance ratio is the ratio of the inert medium's acoustic impedance to that of the combustible medium: $Z = z_i/z_c$. The acoustic impedance of a medium is given by:

$$z = \left\{ \frac{\rho_1 P_1}{2} \left[(\gamma_1 + 1) \frac{P_2}{P_1} + (\gamma_1 - 1) \right] \right\}^{1/2} \tag{6}$$

where ρ , P , and γ are the local density, pressure, and specific heat ratio, respectively. The subscripts 1 and 2 denote unburned and burned conditions, respectively, in the combustible medium, and denote initial and post-transmitted shock conditions, respectively, in the inert medium. Peace and Lu [28] found that the transmission ratio, e.g., the ratio of transmitted shock wave velocity to that the detonation wave velocity ($\Gamma = V_T/V_{CJ}$), was greater than unity for low impedance ratios ($z < 1$, reflected rarefaction) and less than unity for high impedance ratios ($z > 1$, reflected shock). The data provided by Peace and Lu [28] indicate impedance and transmission ratios of approximately 1.45 ± 0.06 and 0.60 ± 0.04 , respectively, for the conditions in the experiments conducted here. Accordingly, the expected transmitted shock wave velocity is approximately 1700 ± 115 m/s.

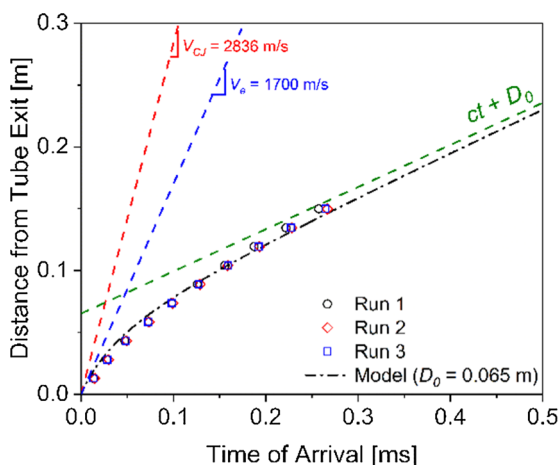


Fig. 7 (Left) Near- and (right) far-field pressure decay data collected for a shock wave transmitted into ambient air from a stoichiometric H_2/O_2 detonation inside of a tube (ID = 1.27 cm). Points correspond

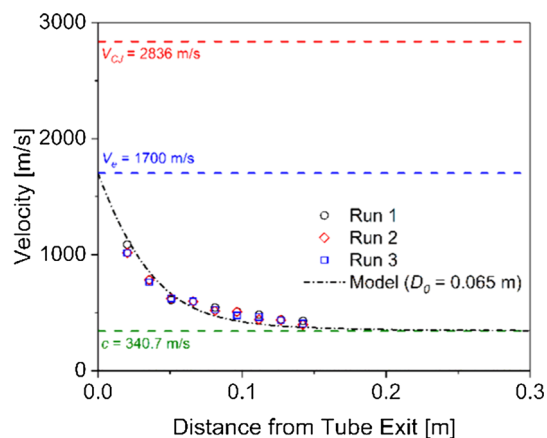
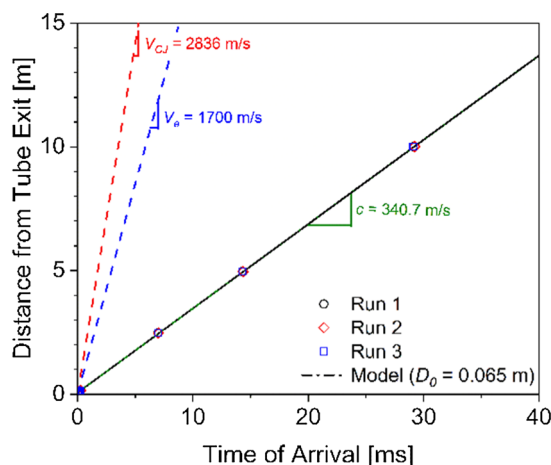


Fig. 8 Near-field velocity decay data from the present study collected for a shock wave transmitted into ambient air from a stoichiometric H_2/O_2 detonation inside of a tube (ID = 1.27 cm). Points correspond to experimental measurements with piezoelectric pressure transducers, and the black dash-dotted line corresponds to the decay model

The final parameter (i.e., the decay coefficient) is empirically determined by fitting (1) to the near-field time-of-arrival data. The near- and far-field pressure data for all experiments are shown in the left and right graphs in Fig. 7, respectively. Similarly, the measured shock wave velocity data, taken between pressure transducers, are shown in Fig. 8. The black dash-dotted line in these figures corresponds to the model with an ambient speed of sound of 340.7 m/s, a shock wave transmission velocity of 1700 m/s, and a decay coefficient of 0.065. In general, the decay model matches the $x-t$ and $v-x$ data well with good coefficients of determination ($R^2=0.988$ and 0.882 , respectively). Most of the error in the model appears to be derived from an inaccurate representation of the shock wave velocity at the tube exit. The shock wave velocity could be influenced by:



to experimental measurements with (left) piezoelectric pressure transducers and (right) free-field microphones. The black dash-dotted line corresponds to the decay model

(1) fuel–gas mixture being pushed out of the open end of the tube by the propagating flame front, or (2) local mixing when the plug is removed from the open end of the tube; however, we believe that both these effects are negligible in the current study because the tube length (5 ft) is much longer than the corresponding DDT run-up distance (~1 ft) and the entire experiment takes place in less than one second from when the plug is removed from the tube. Alternatively, a more complicated mathematical representation may be required to better capture the 3D effects near the tube exit. The lack of relevant data, except for those of Peace and Lu [28], indicates that further work is required in evaluating impedance matching for relevant ranges of impedance ratios and transition geometries.

Equations (4), (5) combined with the measured ambient speed of sound, estimated shock wave exit velocity, and empirical decay coefficient provide a complete analytical representation of the shock wave's history. These relations can be combined with the one-dimensional moving normal shock equations (summarized in the Appendix) [32] to estimate the conditions created by shock wave arrival at any location away from the tube exit, as shown in Fig. 9. The lines correspond to computations completed as described, and solid symbols correspond to static pressure measurements taken by the pressure transducers during experiments. In addition, computations were completed using time-of-flight measurements as a direct input (e.g., instead of (4), (5)) which are shown as open symbols. The good agreement between static pressures predicted with the average shock wave velocity (open symbols) and direct static pressure measurements (solid symbols) indicates the theoretical modeling framework adapted here is technically sound. There is, however, some disagreement between the fully analytical model (red dashed lines) and the direct pressure measurements (solid symbols), so that the static pressure is over- and under-

predicted near and far from the tube exit, respectively. These discrepancies are derived from the imperfect fit of (4), (5) to the time-of-arrival data and, more likely, an inaccurate representation of the shock wave velocity at the tube exit. More explicitly, an inaccurate representation of the shock wave velocity affects the 1D gas-dynamic analysis. In comparison with previous modeling efforts in the literature based on weak/strong shock correlations [20,21] and empirical correlations from data [25], the current modeling efforts include gas-dynamic analyses and should be more accurate.

4 Conclusion

The decay of shock waves transmitted into an open atmosphere from a detonation tube (H_2/O_2 , $\phi=1$, $P=0.1$ MPa) was measured with a new experimental facility. The experiment began with ignition of a reactive gas mixture in a confined tube, DDT occurring in the tube, development of a CJ detonation, transmission of a shock wave into the surrounding atmosphere at the open end of the tube, and the eventual decay of the shock wave to an acoustic wave. The time-of-arrival data in the near and far fields are well described by an oblique asymptote equation with three parameters: the local speed of sound, the velocity of the shock wave exiting the tube, and an empirical decay coefficient. The gas-dynamic equations for a moving normal shock wave were combined with this analytical treatment of the shock wave decay to yield a full description of the conditions immediately behind the shock wave at any distance in front of the detonation tube. Generally, good agreement was observed between the model and the experimental data. Further work is required to establish accurate a priori estimation of the both the shock wave velocity at the tube exit and the decay coefficient for a range of applicable conditions. Additional work

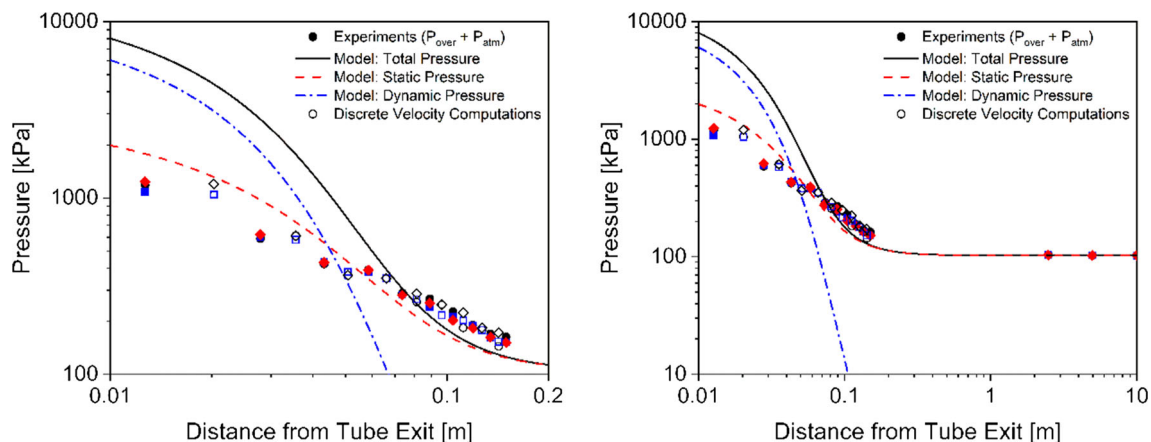


Fig. 9 Pressure conditions behind a shock wave transmitted from a stoichiometric H_2/O_2 detonation tube (ID = 1.27 cm) propagating into an open atmosphere in the (left) near and (right) far fields. Lines correspond

to gas-dynamics model; solid symbols correspond to measurements made with pressure transducers; and open symbols correspond to model computations completed with time-of-flight measurements

is currently being completed to establish similar datasets for larger detonation tubes (ID = 2.54 and 5.08 cm), which will allow for additional more complete analyses.

Acknowledgements This work was sponsored by the O'Donnell Foundation Chair and the Governor's University Research Initiative/Chancellor's Research Initiative (GURI/CRI) at Texas A&M University. Additional support came from the TEES Turbomachinery Laboratory.

Appendix

The model developed here combines (4), (5) with the one-dimensional moving normal shock equations [32], which are summarized in Fig. 10.

Declarations

Conflict of interest The authors declare that they have no conflicts of interest.



Reference Frame: Moving Shock Wave	Reference Frame: Stationary Shock Wave
	
$S_2 = V - a_b M_b$ $M_2 = \frac{S_2}{a_2}$ $\frac{P_2}{P_1} = 1 + \gamma \left(\frac{V S_2}{a_1^2} \right)$ $\frac{P_{02}}{P_2} = \left[1 + \left(\frac{\gamma - 1}{2} \right) \left(\frac{S_2}{a_2} \right)^2 \right]^{1/\gamma - 1}$ $T_2 = T_B$	$S_A = V$ $M_A = \frac{S_A}{a_A}$ $P_A = P_{atm}$ $\frac{P_{0A}}{P_A} = \left[1 + \left(\frac{\gamma - 1}{2} \right) M_A^2 \right]^{1/\gamma - 1}$ $T_A = T_{atm}$
$S_1 = 0$ $M_1 = 0$ $P_1 = P_{atm}$ $P_{01} = P_{atm}$ $T_1 = T_{atm}$	$M_B = \left\{ \left[M_A^2 + \left(\frac{2}{\gamma - 1} \right) \right] \left[\left(\frac{2\gamma}{\gamma - 1} \right) M_A^2 - 1 \right]^{-1} \right\}^{1/2}$ $\frac{P_B}{P_A} = \left(\frac{2\gamma}{\gamma + 1} \right) M_A^2 - \left(\frac{\gamma - 1}{\gamma + 1} \right)$ $\frac{P_{0B}}{P_B} = \left[1 + \left(\frac{\gamma - 1}{2} \right) M_B^2 \right]^{1/\gamma - 1}$ $\frac{T_B}{T_A} = \frac{2(\gamma - 1)}{M_A^2(\gamma + 1)^2} \left[1 + \left(\frac{\gamma - 1}{2} \right) M_A^2 \right] \left[\left(\frac{2\gamma}{\gamma - 1} \right) M_A^2 - 1 \right]$

Fig. 10 Summary of 1D gas-dynamic equations utilized to compute the conditions behind the moving shock wave propagating in an open atmosphere [32]

References

- Oran, E.S., Gamezo, V.N.: Origins of the deflagration-to-detonation transition in gas-phase combustion. *Combust. Flame* **148**(1), 4–47 (2007). <https://doi.org/10.1016/j.combustflame.2006.07.010>
- Morrison, R.B.: A shock tube investigation of detonative combustion. UMM-97, University of Michigan, Ann Arbor (1952)
- Lee, B.H.K.: Detonation-driven shocks in a shock tube. *AIAA J.* **5**(4), 791–792 (1967). <https://doi.org/10.2514/3.4065>
- Yu, H.R., Esser, B., Lenartz, M., Gronig, H.: Gaseous detonation driver for a shock tunnel. *Shock Waves* **2**(1), 245–254 (1992). <https://doi.org/10.1007/BF01414760>
- Hongru, Y.: Oxyhydrogen combustion and detonation driven shock tube. *Acta Mech. Sinica* **15**(2), 97–107 (1999). <https://doi.org/10.1007/BF02485874>
- Lu, F.K., Wilson, D.R., Bakos, R.J., Erdos, J.I.: Recent advances in detonation techniques for high-enthalpy facilities. *AIAA J.* **38**(9), 1676–1684 (2000). <https://doi.org/10.2514/2.1153>
- Olivier, H., Jiang, Z., Yu, H.R., Lu, F.K.: Detonation-driven shock tubes and tunnels. In: Lu, F., Marren, D. (eds.) *Advanced Hypersonic Test Facilities*. AIAA, Reston, VA (2002). <https://doi.org/10.2514/5.9781600866678.0135.0203>
- Lu, F.K., Wilson, D.R.: Detonation driver for enhancing shock tube performance. *Shock Waves* **12**, 457–468 (2003). <https://doi.org/10.1007/s00193-003-0186-1>
- Li, J., Chen, H., Yu, H.: A chemical shock tube driven by detonation. *Shock Waves* **22**(1), 351–362 (2012). <https://doi.org/10.1007/s00193-012-0374-y>
- Armstrong, J.: Design of a free field blast simulating shock tube. MS Thesis, University of Ottawa (2015)
- Luo, K., Wang, Q., Li, J., Li, J., Zhao, W.: Numerical modeling of a high-enthalpy shock tunnel driven by gaseous detonation. *Aerosp. Sci. Technol* **104**(1), 1–8 (2020). <https://doi.org/10.1016/j.ast.2020.105958>
- Jiang, Z., Li, J., Hu, Z., Liu, Y., Yu, H.: On theory and methods for advanced detonation-driven hypervelocity shock tunnels. *Natl. Sci. Rev.* **7**(7), 1198–1207 (2020). <https://doi.org/10.1093/nsr/nwaa050>
- Paterson, S.: Contact transmission of detonation. *Symp. (Int.) Combust.* **4**(1), 468–471 (1953). [https://doi.org/10.1016/S0082-0784\(53\)80065-2](https://doi.org/10.1016/S0082-0784(53)80065-2)
- Fickett, W.: Motion of an explosion-induced plane shock wave. *Q. Appl. Math.* **32**(1), 71–84 (1974). <https://doi.org/10.1090/qam/99688>
- Thomas, G.O., Sutton, P., Edwards, D.H.: The behavior of detonation waves at concentration gradients. *Combust. Flame* **84**(3), 312–322 (1991). [https://doi.org/10.1016/0010-2180\(91\)90008-Y](https://doi.org/10.1016/0010-2180(91)90008-Y)
- Sochet, I., Lamy, T., Brossard, J., Vagilo, C., Cayzac, R.: Critical tube diameter for detonation transmission and critical initiation energy of spherical detonation. *Shock Waves* **9**(1), 113–123 (1999). <https://doi.org/10.1007/s001930050146>
- Kato, S., Hashimoto, S., Uemichi, A., Kasahara, J., Matsuo, A.: Propagation characteristics of shock waves driven by gaseous detonation waves. *Shock Waves* **20**(1), 479–489 (2010). <https://doi.org/10.1007/s00193-010-0279-6>
- Bertrand, B.P., Matthews, W.T.: Overpressures and durations of shock waves emerging from open-ended shock tubes. AD-0633161, US Army Aberdeen Proving Ground, MD (1965)
- Schmidt, E., Duffy, S.: Noise from shock tube facilities. 23rd AIAA Aerospace Sciences Meeting, Reno, NV, AIAA Paper 1985-0049 (1985). <https://doi.org/10.2514/6.1985-49>
- Allgood, D.C.: An experimental and computational study of pulse detonation engines. PhD Thesis, University of Cincinnati (2004)
- Glaser, A.J., Caldwell, N., Gutmark, E.: A Fundamental study on the acoustic behavior of pulse detonation engines. 45th AIAA Aerospace Sciences Meeting, Reno, NV, AIAA Paper 2077-0444 (2007). <https://doi.org/10.2514/6.2007-444>
- Xu, G., Weng, C.S., Li, N., Huang, X.L.: Investigation of thrust augmentation and acoustic performance by ejectors on PDE. *Int. J. Turbo Jet Eng.* **33**(1), 19–26 (2016). <https://doi.org/10.1515/tjj-2015-0002>
- Huang, X., Weng, C., Li, N., Xu, G.: Experimental study of acoustic behavior of three-tube PDE system in near-field. *Explos. Shock Waves* **36**(5), 633–639 (2016). [https://doi.org/10.11883/1001-1455\(2016\)05-0633-07](https://doi.org/10.11883/1001-1455(2016)05-0633-07)
- Kang, Y., Li, N., Weng, C.S., Wang, C.W.: Acoustic characteristics of pulse detonation engine with ellipsoidal reflector. *Chinese Phys. B.* **27**(10), 1–11 (2018)
- Anand, V., Glaser, A., Gutmark, E.: Acoustic characterization of pulse detonation combustors. *AIAA J.* **56**(7), 2806–2815 (2018). <https://doi.org/10.2514/1.J056204>
- Xu, G.Y., Wang, C.G., Zhu, Y.F., Li, H.Y., Gong, L.K., Wang, J.N.: Study on influence of diameter on detonation acoustic characteristics of pulse detonation engine. *Int. J. Turbo Jet Eng.* **37**(1), 1–8 (2020). <https://doi.org/10.1515/tjj-2020-0003>
- Pack, D.C.: The reflection and transmission of shock waves I: The reflection of a detonation wave at a boundary. *Philos. Mag.: J. Theor. Exp. Appl. Phys.* **2**(14), 182–188 (1957). <https://doi.org/10.1080/14786435708243807>
- Peace, J.T., Lu, F.K.: Detonation-to-shock wave transmission at a contact discontinuity. *Shock Waves* **28**(5), 981–992 (2018). <https://doi.org/10.1007/s00193-018-0804-6>
- Dorofeev, S.B., Sidorov, V.P., Kuznetsov, M.S., Dvoynishnikov, A.E., Alekseev, V.I., Efimenko, A.A.: Air blast and heat radiation from fuel-rich mixture detonations. *Shock Waves* **6**(1), 21–28 (1996). <https://doi.org/10.1007/BF02511401>
- Lee, J.H.S.: Deflagration-to-detonation transition. In: *The Detonation Phenomenon*. Cambridge University Press, New York (2008). <https://doi.org/10.1017/CBO9780511754708.009>
- Ciccarelli, G., Boccio, J.L., Ginsberg, T., Finfrock, C., Gerlach, L., Tagawa, H., Malliakos, A.: The effect of initial temperature on flame acceleration and deflagration-to-detonation transition phenomenon. BNL-NUREG-52515, U.S. Nuclear Regulatory Commission, Washington, DC (1998)
- John, J.E., Keith, T.G.: Moving normal shockwaves. In: *Gas Dynamics*. Pearson Education, Upper Saddle River (2006)

Publisher's Note Springer Nature remains neutral with regard to jurisdictional claims in published maps and institutional affiliations.